Cobalt-based ZIF-68 and ZIF-69 as the precursors of non-platinum electrocatalysts for oxygen reduction

Yulia A. Pimonova,*[a,b] Tatiana A. Lastovina,*[a,c] Andriy P. Budnyk,[c]
Egor A. Kudryavtsev[d] and Maxim N. Yapryntsev[d]

[a] *International Research Center 'Smart Materials', Southern Federal University, 344090 Rostov-on-Don,
Russian Federation. E-mail: lastovina@sfedu.ru*
[b] *Department of Chemistry, Southern Federal University, 344090 Rostov-on-Don, Russian Federation*
[c] *Southern Scientific Center, Russian Academy of Sciences, 344006 Rostov-on-Don, Russian Federation*
[d] *Belgorod National Research University, 308015 Belgorod, Russian Federation*

We report the microwave-assisted synthesis of Co-based ZIF-68 and ZIF-69 zeolitic imidazolate frameworks, which were enriched with iron(II) acetate and 1,10-phenanthroline and then pyrolyzed to form heterogeneous catalysts. The materials demonstrated high activity in oxygen reduction and suitability as Pt-free catalysts for low-temperature fuel cells.
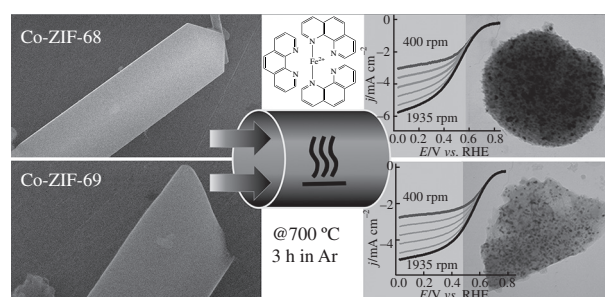
The efficiency of low-temperature hydrogen–oxygen fuel cells is limited by the rate of a cathodic oxygen reduction reaction (ORR), and catalysts are used to compensate the problem. Since efficient Pt-containing catalysts[1] are extremely expensive and tend to degrade, attention was focused on nonprecious metal ones, including different doped catalysts. Recently, active carbons prepared through the heat treatment of biowaste[2] or metal-organic frameworks (MOFs)[3–7] were proposed because they can serve simultaneously as templates and carbon precursors.[6] Zeolitic imidazolate frameworks (ZIFs) are favorable carbon precursors due to their tunable and variable pore types and sizes; the imidazole linkers act as a source of nitrogen.[3] ZIF-8 and ZIF-67, which are catalytically active, have been actively exploited for the preparation of carbonaceous catalysts for ORR.[8] Isostructural ZIF-68 and ZIF-69 are much less studied in this regard[5] although they were found efficient in H_2 and CO_2 sorption.[9] The aim of this work was to study carbons derived from the structures hosting cobalt ions instead of zinc because cobalt and cobalt oxide nanoparticles (NPs) are active toward ORR.[3,10] As in ZIF-8/67, Zn and Co ions are interchangeable in ZIF-68 and ZIF-69 without structure alternation, as illustrated by the production of bimetallic frameworks.[3,11]

We prepared the catalysts according to a three-step approach developed for ZIF-8/67 and reported elsewhere.[12] First, we synthesized Co-based ZIF-68 (CoZ-68) and ZIF-69 (CoZ-69) structures by a microwave-assisted solvothermal method at 135 °C for 3 h. Second, we introduced iron and increased the nitrogen content by contacting MOFs with a Fe[II]–phenanthroline complex. Finally, we pyrolyzed MOFs at 700 °C for 3 h in argon to obtain carbonaceous catalysts.[†] The CoZ-68 and CoZ-69 MOFs and the resulting carbons, denoted as CoZ-68-C and CoZ-69-C, respectively, were characterized by different experimental techniques.[‡]

The morphology of products was observed by electron microscopy (Figure 1). The SEM image of CoZ-68 [Figure 1(*a*)] demonstrates rod-shaped crystallites with an average length of 9–11 μm and a width of 2–4 μm. Note that a number of crystallites seems broken, while some large hexagonal rods propagate up to 21 μm. In addition to the rods, there are small round-like particles (Figure S1, see Online Supplementary Materials). The STEM-EDX mapping (Figure S2) demonstrated a homogeneous distribution of Co, Fe, C, and N across the material. As for CoZ-69 [Figure 1(*b*)], smaller elongated crystallites with rounded ends and average dimensions of 4×1 μm were observed.

---

† Commercial reagents were used as received. (i) *Synthesis of CoZ-68*. $Co(NO_3)_2 \cdot 6H_2O$ (0.2 mmol) was dissolved in DMF (1 ml) and a composition of 2-nitroimidazole (0.3 mmol) and benzimidazole (0.2 mmol) was dissolved in DMF (2.5 ml). Afterward, the former was added to the latter dropwise. The mixture was loaded in a Discover SP microwave reactor (CEM) and left to react at 135 °C for 3 h with stirring. The red-purple precipitate obtained was washed once with DMF and thrice with methanol and dried overnight at 50 °C. (ii) *Synthesis of CoZ-69*. 2-Nitroimidazole (1.2 mmol), 5-chlorobenzimidazole (1.2 mmol) and $Co(NO_3)_2 \cdot 6H_2O$ (0.6 mmol) were dissolved in DMF (12 ml). The mixture was placed in a Discover SP and left to react at 120 °C for 2 h with stirring. The resulting dark purple precipitate was triply washed with methanol and dried overnight at 60 °C. (iii) *Impregnation with Fe[II]–phenanthroline*. $Fe(OAc)_2$ (0.005 g) and 1,10-phenanthroline (0.0315 g) were dissolved in ethanol (5 ml) to form a red solution, and the ZIF powder (0.125 g) was added. The mixture was sonicated for 30 min, stirred for 1 h, and dried at 60 °C. (iv) *Pyrolysis*. ZIFs were heated in a tube furnace (Nabertherm) to 700 °C with a rate of 10 °C min⁻¹ and kept for 3 h in an Ar flow.

‡ X-ray diffraction (XRD) analysis was performed on a SmartLab (Rigaku) diffractometer. Scanning electron microscopy (SEM) was carried out on a Supra 25 (Zeiss) microscope. Transmission electron microscopy (TEM) was performed on a JEM-2100 (JEOL) microscope operated at an accelerating voltage of 200 kV.
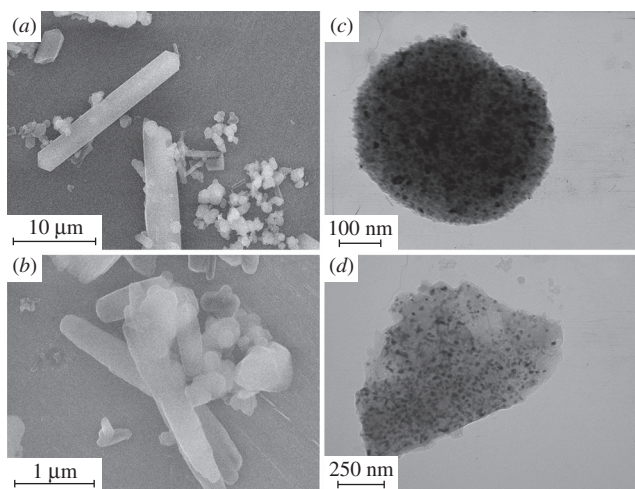
Figure 1 SEM images of (*a*) CoZ-68 and (*b*) CoZ-69. TEM images of (*c*) CoZ-68-C and (*d*) CoZ-69-C pyrolyzed powders.

Carbonaceous materials were studied by TEM. Both CoZ-68-C and CoZ-69-C consist of carbonaceous globules containing metal NPs (see Figure 1). The particle size distribution (Figure S3) covers a range of 4–22 nm. For CoZ-68-C, it peaks around 8 nm with a substantial contribution from 6–16 nm particles (Figure S1). There is a well-defined maximum at 16–18 nm in particle size distribution histogram for CoZ-69-C [Figure S1(*b*)]. The occurrence of relatively large metal NPs can be due to the absence of a separating agent. Zinc is known to play this role in bimetallic ZIFs.[3]

The structure of the samples was assessed with powder XRD (Figure 2). The synthesized MOFs are highly crystalline
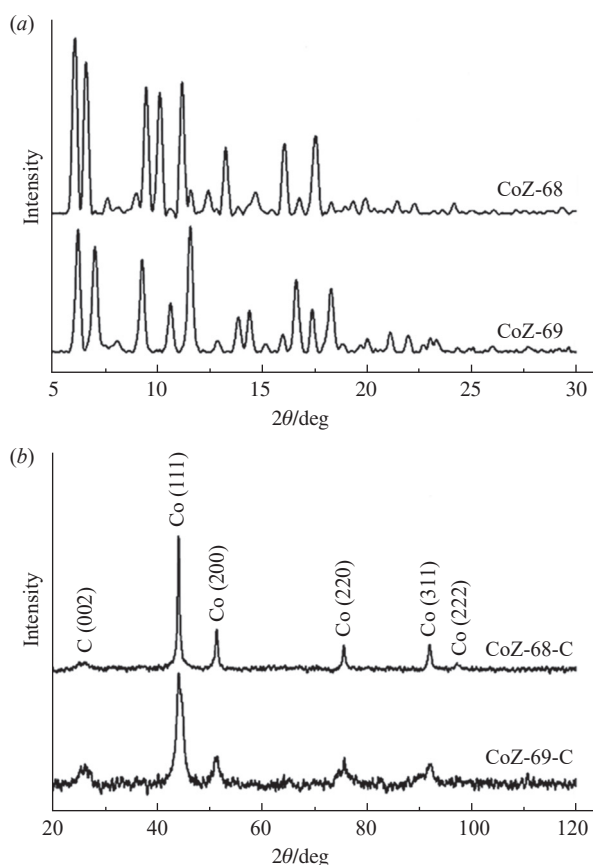
[Figure 2(*a*)], and their diffraction patterns are consistent with published data for ZIF-68 and ZIF-69.[7] The diffraction picture of carbonized materials [Figure 2(*b*)] contains contributions from graphitized carbon and metal NPs formed during the high-temperature treatment. A broad peak at 26.1° evidences the graphite structure in the spatial symmetry group *Fmmm* (69) (database card no. PDF-2-9000046). At lager 2θ angles, there are reflections from a crystalline structure of cobalt in the spatial symmetry group *Fm*-3*m* (225) (database card no. PDF-2-9008466), considering its relatively high loading in respect to iron. The lattice parameters for metal NPs in CoZ-68-C and CoZ-69-C were evaluated as 3.5459 and 3.5485 Å, respectively. The values are close to that of pure cobalt, 3.548 Å. Although, we cannot exclude the doping of cobalt NPs with iron. No diffraction peaks remained from the original ZIFs, confirming the complete destruction of the ZIF structure. The average sizes of metal NPs were 9.2 and 18.2 nm for CoZ-68-C and CoZ-69-C, respectively.

The Raman spectra of pyrolyzed samples (Figure S3) exhibit characteristic bands at 1349 and 1591 cm^{-1}, which are the disorder-induced D-band and the symmetry-allowed G-band of carbon, respectively. Their intensities are almost equal due to a high level of structure imperfection. Carbon is sp^3-hybridized, and it does not form graphite/graphene structures in appreciable quantities.

The electrochemical tests included cyclic voltammetry (CV) and linear sweep voltammetry (LSV) in a potential range of 1.2–0.03 V *vs*. RHE with scan rates of 20 and 5 V s^{-1}, respectively.[§] Prior to the CV measurements in an O$_2$ atmosphere at a rotation rate of 1600 rpm, the pre-cycling was performed
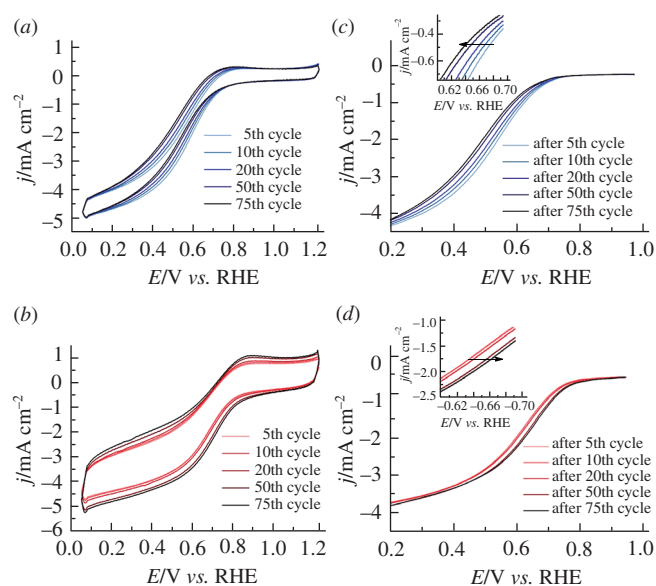

Figure 2 XRD patterns of (*a*) as-synthesized MOFs and (*b*) pyrolyzed carbons.

Figure 3 CV curves for (*a*) CoZ-68-C and (*b*) CoZ-69-C collected in 0.1 M HClO$_4$ at a scan rate of 20 mV s^{-1}, 25 °C in an O$_2$ atmosphere at a rotation rate of 1600 rpm and the LSV curves for (*c*) CoZ-68-C and (*d*) CoZ-69-C.
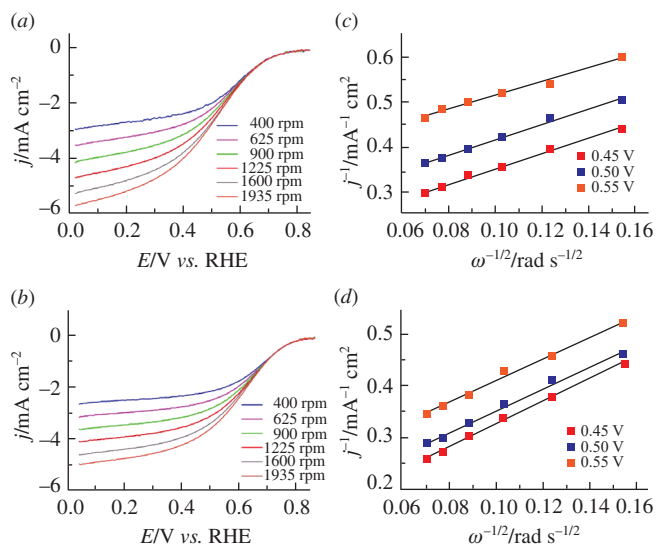
Figure 4 LSV curves at different sweep rates for (*a*) CoZ-68-C and (*b*) CoZ-69-C and the Koutecky–Levich plots for (*c*) CoZ-68-C and (*d*) CoZ-69-C.

under the same conditions but in an Ar atmosphere with RDE off. According to the CV curves (Figure 3), the potentials of CoZ-68-C and CoZ-69-C changed from 0.427 to 0.374 or from 0.520 to 0.552 V, respectively, in the 5th and 75th cycles. The LSV data [Figures 3(*c*,*d*)] clearly demonstrate that the half-wave potential of CoZ-69-C increased, while that of CoZ-68-C decreased. During the test, CoZ-69-C demonstrated superior absolute potential values and a shift toward higher potentials. This fact indicated that the catalyst surface was improved rather than degraded over cycling (as for CoZ-68-C).

The ORR kinetics was studied using LSV at various sweep rates of RDE [Figures 4(*a*,*b*)] and calculations according to the Koutecky–Levich equation (see Online Supplementary Materials). The linear and almost parallel Koutecky–Levich plots [Figures 4(*c*,*d*)] imply the first order of reaction. The electron transfer numbers from 5.0 to 5.6 V for CoZ-68-C and from 3.9 to 4.1 V for CoZ-69-C were calculated according to these plots at 0.45–0.55 V. With no doubt, the four-electron pathway of ORR can be defined for CoZ-69-C. On the contrary, the activity of CoZ-68-C is impaired by an unknown side reaction, which may include the formation of hydrogen peroxide. The intense ORR activity of CoZ-69-C is also reflected by the higher onset and half-wave potentials. The respective values are 0.964 and 0.634 V in comparison to 0.852 and 0.583 V for CoZ-68-C.

Thus, we synthesized carbonaceous electrocatalysts from sacrificial cobalt-based ZIF-68 and ZIF-69 MOFs. The catalysts demonstrated good electrocatalytic activity in ORR with some prevalence of CoZ-69-C. Moreover, the electron transfer number for CoZ-69-C was extremely close to 4 evidencing an efficient pathway without a by-product.

Online Supplementary Materials
Supplementary data associated with this article can be found in the online version at doi: 10.1016/j.mencom.2019.09.022.

References

1 (*a*) A. B. Kuriganova, I. N. Leontyev, O. A. Maslova and N. V. Smirnova, *Mendeleev Commun.*, 2018, **28**, 444; (*b*) I. N. Leontyev, D. V. Leontyeva, A. B. Kuriganova, Yu. V. Popov, O. A. Maslova, N. V. Glebova, A. A. Nechitailov, N. K. Zelenina, A. A. Tomasov, L. Hennet and N. V. Smirnova, *Mendeleev Commun.*, 2015, **25**, 468; (*c*) V. E. Guterman, S. V. Belenov, T. A. Lastovina, E. P. Fokina, N. V. Prutsakova and Ya. B. Konstantinova, *Russ. J. Electrochem.*, 2011, **47**, 933 (*Elektrokhimiya*, 2011, **47**, 997).
2 D. V. Chernysheva, Y. A. Chus, V. A. Klushin, T. A. Lastovina, L. S. Pudova, N. V. Smirnova, O. A. Kravchenko, V. M. Chernyshev and V. P. Ananikov, *ChemSusChem*, 2018, **11**, 3599.
3 B. N. Bhadra, A. Vinu, C. Serre and S. H. Jhung, *Mater. Today*, 2019, **25**, 88.
4 T. Lastovina, J. Pimonova and A. Budnyk, *J. Phys. Conf. Ser.*, 2017, **829**, 012007.
5 T. Palaniselvam, B. P. Biswal, R. Banerjee and S. Kurungot, *Chemistry*, 2013, **19**, 9335.
6 Q. Wang, W. Xia, W. Guo, L. An, D. Xia and R. Zou, *Chem. Asian J.*, 2013, **8**, 1879.
7 X. Wang, J. Zhou, H. Fu, W. Li, X. Fan, G. Xin, J. Zheng and X. Li, *J. Mater. Chem. A*, 2014, **2**, 14064.
8 (*a*) A. V. Stepanov, K. E. Mel'nik, V. I. Isaeva, G. I. Kapustin, V. V. Chernyshev and V. V. Veselovsky, *Mendeleev Commun.*, 2018, **28**, 88; (*b*) T. Lastovina, A. Budnyk, Yu. Pimonova, A. Bugaev and V. Dmitriev, *Int. J. Hydrogen Energy*, 2019, **44**, 23010; (*c*) Z. Zhu, C. Chen, M. Cai, Y. Cai, H. Ju, S. Hu and M. Zhang, *Mater. Res. Bull.*, 2019, **114**, 161.
9 (*a*) T. Panda, K. M. Gupta, J. Jiang and R. Banerjee, *CrystEngComm*, 2014, **16**, 4677; (*b*) T. Pham, K. A. Forrest, H. Furukawa, M. Russina, A. Albinati, P. A. Georgiev, J. Eckert and B. Space, *J. Phys. Chem. C*, 2017, **121**, 1723; (*c*) S. Van der Perre, T. Van Assche, B. Bozbiyik, J. Lannoeye, D. E. De Vos, G. V. Baron and J. F. M. Denayer, *Langmuir*, 2014, **30**, 8416; (*d*) L. Yang, L. Yu, G. Diao, M. Sun, G. Cheng and S. Chen, *J. Mol. Catal. A*, 2014, **392**, 278.
10 X. Wen, X. Yang, M. Li, L. Bai and J. Guan, *Electrochim. Acta*, 2019, **296**, 830.
11 D. Zhao, X. Zhu, N. Wang, B. Lu, L. Li and S. Chen, *Mater. Today*, 2019, **11**, 253.
12 T. A. Lastovina, A. P. Budnyk, Y. A. Pimonova, A. L. Bugaev, A. G. Fedorenko and V. P. Dmitriev, *Electrochem. Commun.*, 2018, **88**, 83.